Int. J. Nanoelectronics and Materials **9** (2016) 67-84

Simulation Study of 2D Electron Density in Primed and Unprimed Subband Thin-Body Double-Gate Nano-MOSFET of Three Different Thicknesses and Two Temperature States

Ooi Chek Yee[1,*], *Lim Soo King*[2]

[1]*Faculty of Information and Communication Technology, UniversitiTunku Abdul Rahman, Jalan Universiti, Bandar Barat, 31900 Kampar, Perak, Malaysia.*
[2]*Lee Kong Cian Faculty of Engineering and Science, UniversitiTunku Abdul Rahman, Jalan Genting Kelang, 53300 Setapak, Kuala Lumpur, Malaysia.*

Received 30 Dec. 2014; Revised 7 April 2015; Accepted 6 May 2015

Abstract

This paper presents a theoretical simulation study for electrical characteristics of double-gate (DG) nano-MOSFET at equilibrium thin-body condition. The electrical characteristics under studied are subband energy (including unprimed and primed subbands) as well as 2D electron density at 77K and 300K ambient temperatures. The values of silicon body thickness T_{Si} are 1.0nm, 1.5nm and 2.0nm. The electron transport models used in NanoMOS simulation tool covered quantum model and classical model. The simulation output data are discussed based on quantum effects and property of particle-wave duality of electron. In quantum model, low temperature 77K exhibits wave interference effects whereas high temperature 300K exhibits particle nature. This is due to inelastic electron-phonon collisions (quantized lattice vibrations) at high temperature. These inelastic collisions cause dephasing events. This decoherence causes nanodevices to exhibit classical behavior and is the most challenging problem faces when developing quantum computers. Currently, quantum computing is still in early development state. This study attempts to relate silicon-based nanodevice theory with a technology for quantum information processing. Quantum computers may become reality by incorporating the silicon semiconductor technology used by current electronic industry. The most advanced quantum computers have been established only in very small systems, such as an array of individual phosphorus donor atoms in pure silicon lattice in Kane quantum computer. So, the motivation for this study is to scale the quantum computer systems to very large sizes by using silicon nano-MOSFET. However, at large quantum computer systems, quantum errors occur due to decoherence. To solve this problem, large size quantum computers made from silicon nano-MOSFET should operate at cryogenic temperature (extremely low temperature) where electrons behave like wave. Quantum mechanics enables nanodevice systems to store and manipulate a vast amount of information. Therefore, nanodevice is simulated in this paper in order to examine quantum computer.

Keywords: ballistic transport, classical behavior, nanometer, temperature effects, wave nature, particle.
PACS: 73.30.+y, 73.40.Ns, 73.40.-c.

[*]) For Correspondence, Tel: + (60) 5 4688888 Ext: 4420, Fax: + (60) 5 4661672, E-mail: ooicy@utar.edu.my

1. Introduction

Semiconductor devices such as nano-MOSFET operate by controlling the flow of electron through the channel. The movement of electrons within the nano-MOSFET could be particle and wave nature [1,2,3]. Particle nature of electron movement is described by Boltzmann Transport Equation (BTE) whereas quantum model is used to describe the wave nature of electron movement [4,5]. This particle-wave duality property of electron can be observed by examining the effects of temperature variation on the electron distribution in the channel of nano-MOSFET [4,5].

Quantum computers can be the ideal devices for cracking modern encryption codes and searching through huge databases. Silicon-based quantum computing has long coherence times which enable quantum computer computation to finish before quantum state decoheres. In normal nanosystems, temperature variations can affect phase coherence. Since phonon energy is greater at higher temperature, thermal decoherence occurs at 300K high temperature in this simulation project. Quantum computations in nanosystems are preferably operated at cryogenic temperature (which is extremely low temperature like 77K in this simulation project). Silicon nano-MOSFET with individual phosphorus donor atoms embedded in pure silicon lattice is used to study silicon-based quantum computing in this research project [6,7,8,9].

As transistors in microchips approach the atomic scale, ideas from quantum computing are likely to become relevant for classical computing. Quantum mechanics enables quantum computer to store and manipulate a vast amount of information. If quantum computer can be implemented with nanodevices, it would be a magic computer because quantum computers are exceptionally fast at some specific tasks [10]. This realization covers physical principles in nanotechnology, quantum mechanics, solid state physics and chemistry which are outside of the traditional electron physics disciplines [6].

In this paper, simulation results of temperature 300K and 77K are compared because at 77K (extremely low temperature) electron transport in nano-MOSFET with quantum model behaves like wave where constructive interference and destructive interference of quantum particles formed the quantum computer algorithm [10]. At room temperature 300K quantum interference disappears [5]. The nanometer values of silicon body thickness are chosen such that quantum energy levels splitting become significant and thus quantum mechanics principle can be applied to explain electron movement [11,12]. These nanometer dimensions are important since quantum mechanics is needed to describe quantum computer. In bulk silicon material, there are too many energy levels such that these energy levels can't be distinguished. When quantum energy levels splitting occur in nanometer silicon body, primed and unprimed subbands occur. However, the unprimed subbands with heavier longitudinal electron mass will have lower bound-state energies as compared to primed subbands. Therefore, 1st unprimed subband primarily occupied by electrons and thus when performing simulation analysis, it is enough to analyze electron movement with this 1st unprimed subband [4,5].

2. Theory

DG nano-MOSFET with silicon channel length at 10nm studied in this paper is approaching the ballistic transport regime since the phonon mean free path scattering for electron in silicon is 76Å (7.6nm) [13]. When the channel of this nano-MOSFET is thin enough (less than 5nm, typically), the energy levels splitting will be significantly larger than thermal voltage (0.025eV at 300K), and electrons are only able to occupy the bottom

subbands without hopping to higher levels. In this case, Schrödinger equation can be used to solve for wavefunction which in turn is used to obtain electron spatial distribution. The conduction band in silicon consists of two sets of subbands that are unprimed subbands and primed subbands. Owing to the heavier effective mass electrons, unprimed subbands have relatively lower bound state energies as compared to the lighter effective mass electrons in primed subband. In real simulation, the lowest few subbands are sufficient to produce accurate results because electrons basically occupied these few lower energy subbands [4]. According to ZhibinRen work [5], in the Possion solver used in the simulation tool, the electron density, n_i for the unprimed and primed subbands is given by

$$n_i = n_{2Di}\ln\left(1 + e^{(E_F - E_i)/k_B T}\right) \quad (1)$$

where n_{2Di}=a constant with 2D dimensions for subband i
E_F = energy of the Fermi level
E_i= energy of conduction band for subband i
k_B= Boltzmann constant
T= Temperature

As cited in reference [14], when letting $\eta_0 = (E_F - E_i)/k_B T$ at gate biasing voltage V_G = drain biasing voltage V_{DD}, the following simplification hold

$$\ln(1 + e^{\eta_0}) \approx \eta_0 \quad (2)$$

From equation (1) and equation (2), at fixed temperature T, n_{2Di} is fixed for subband i, so

$$n_i \propto \left(\frac{E_F - E_i}{k_B T}\right) \quad (3)$$

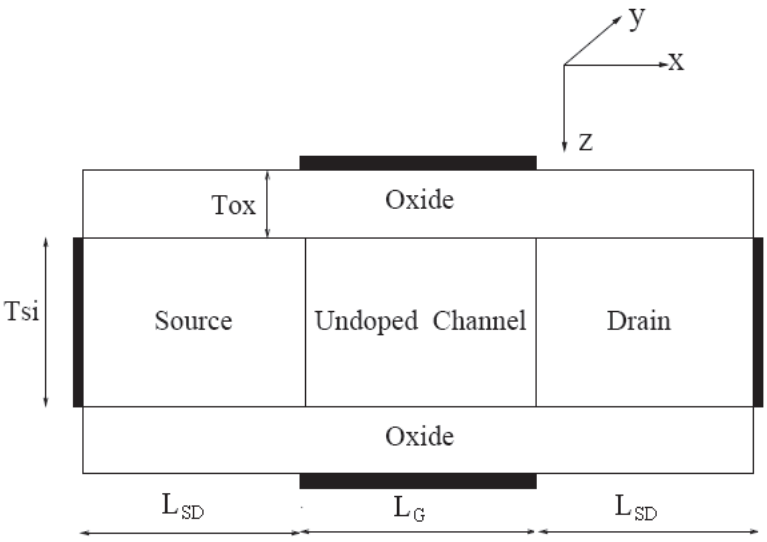

Fig. 1: 2D structural design of DG nano-MOSFET with heavily n+-doped source/drain reservoirs.

Figure 1 shows the 2D structural design of DG nano-MOSFET. Consider the electron movement in a 2D dimension region of the channel, L_Z (channel thickness) x L_X (device length), the 2D Schrödinger equation is given by

$$\left(-\frac{\hbar^2}{2m^*}\left(\frac{\partial^2}{\partial x^2}+\frac{\partial^2}{\partial z^2}\right)-E\right)\psi(x,z)=0 \tag{4}$$

where $\hbar$ = reduced Planck's constant
m^* = electron effective mass (unprimed and primed subband)
E= electron energy
$\psi(x,z)$ = wavefunction

The references for the mathematical descriptions in this section are listed in [6,15,16]. According to reference [6], $\psi(x,z)$ is given by the following product solution

$$\psi(x,z)=\psi_x(x)\psi_z(z) \tag{5}$$

Equation (4) becomes

$$\left(\frac{1}{\psi_x}\frac{\partial^2}{\partial x^2}\psi_x+\frac{1}{\psi_z}\frac{\partial^2}{\partial z^2}\psi_z+\frac{2m^*}{\hbar^2}E\right)=0 \tag{6}$$

The time-dependent wavefunction for an electron is then given by

$$\Psi(\mathbf{r},t)=\psi(\mathbf{r})e^{-\frac{iEt}{\hbar}}=A_0e^{i\mathbf{k}\cdot\mathbf{r}}e^{-\frac{iEt}{\hbar}} \tag{7}$$

where $\mathbf{r}$ = position vector = $a_x x + a_z z$ (in rectangular coordinates; a is unit vector)
$\mathbf{k}$ = wavevector = $a_x k_x + a_z k_z$

The time-independent wavefunction is obtained by putting t=0,

$$\Psi(\mathbf{r},0)=\psi(\mathbf{r}) \tag{8}$$

The boundary conditions for the Schrödinger equation are given by

$$\psi_x(0)=\psi_x(L_x)=0 \tag{9a}$$

$$\psi_z(0)=\psi_z(L_z)=0 \tag{9b}$$

The 2D Schrödinger equation in equation (4) has the following solutions

$$\psi_x(x)=A_x\sin(k_x x)+B_x\cos(k_x x) \tag{10a}$$

$$\psi_z(z)=A_z\sin(k_z z)+B_z\cos(k_z z) \tag{10b}$$

The 2D Schrödinger equation in equation (4) can be written as

$$\left(-\frac{\hbar^2}{2m^*}\left(\frac{\partial^2}{\partial x^2}+\frac{\partial^2}{\partial z^2}\right)\right)\psi(x,z)=E\psi(x,z) \tag{11}$$

Equation (10a) and (10b) are clearly energy eigenfunctions of an eigenfunction of

$$H = \left(-\frac{\hbar^2}{2m^*}\left(\frac{\partial^2}{\partial x^2} + \frac{\partial^2}{\partial z^2}\right)\right) \tag{12}$$

where

$$k_x^2 = \frac{2m^*E}{\hbar^2} \tag{13a}$$

$$k_z^2 = \frac{2m^*E}{\hbar^2} \tag{13b}$$

Since the probability of finding an electron outside the nano-MOSFET is zero (which indicates that the electron is only confined in the 2D nano-MOSFET device), thus at the region outside the 2D device $\psi_x(x) = 0$ and $\psi_z(z) = 0$. Therefore, this 2D nano-MOSFET structure forms a quantum well which is important in nanoelectronics devices because these nanometer devices usually confine electrons in nanoscopic spaces.

Considering $\psi_x(x)$, from boundary condition in equation (9a), equation (10a) can be solved to obtain

$$B_x = 0$$

$$k_x = \frac{n_x\pi}{L_x} \qquad n_x \text{ is quantum number}$$

and so the wavefunction is thus

$$\psi_n(x) = A_x \sin\left(\frac{n_x\pi}{L_x}x\right) \tag{14}$$

From the fact that the electron must be within the 2D device at any moment t,

$$\int_0^{L_x} \left|\psi_n(x)\right|^2 dx = 1 \tag{15}$$

which is normally used to normalize Schrödinger equation's solution and thereby obtaining

$$A_x = \sqrt{\frac{2}{L_x}}$$

and resulting in

$$\psi_n(x) = \sqrt{\frac{2}{L_x}} \sin\left(\frac{n_x\pi}{L_x}x\right) \tag{16}$$

or

$$\Psi_n(x,t) = \left(\frac{2}{L_x}\right)^{1/2} \sin\left(\frac{n_x\pi}{L_x}x\right) e^{-iE_nt/\hbar} \tag{17}$$

Repeating the above procedure for $\psi_z(z)$ and resulting in

$$B_z = 0$$

$$k_z = \frac{n_z \pi}{L_z} \qquad n_z \text{ is quantum number}$$

$$\psi_n(z) = A_z \sin\left(\frac{n_z \pi}{L_z} z\right) \tag{18}$$

$$\int_0^{L_z} \left|\psi_n(z)\right|^2 dz = 1 \tag{19}$$

$$A_z = \sqrt{\frac{2}{L_z}}$$

$$\psi_n(z) = \sqrt{\frac{2}{L_z}} \sin\left(\frac{n_z \pi}{L_z} z\right) \tag{20}$$

$$\Psi_n(z,t) = \left(\frac{2}{L_z}\right)^{1/2} \sin\left(\frac{n_z \pi}{L_z} z\right) e^{-iE_n t/\hbar} \tag{21}$$

From equation (5)

$$\psi(x,z) = \left(\sqrt{\frac{2}{L_x}} \sin\left(\frac{n_x \pi}{L_x} x\right)\right)\left(\sqrt{\frac{2}{L_z}} \sin\left(\frac{n_z \pi}{L_z} z\right)\right) = \left(\frac{4}{L_x L_z}\right)^{1/2} \sin\left(\frac{n_x \pi}{L_x} x\right) \sin\left(\frac{n_z \pi}{L_z} z\right) \tag{22}$$

which have two quantum numbers n_x and n_z. These quantum numbers indicate the state of the electron where different combinations of these quantum numbers indicate different states. The allowed discrete values of energy are given by

$$E_{n_x,n_z} = \frac{\hbar^2 \pi^2}{2m^*}\left(\left(\frac{n_x}{L_x}\right)^2 + \left(\frac{n_z}{L_z}\right)^2\right) \tag{23}$$

Degenerate is the situation where states with different quantum numbers but have the same energy.

In 2D rectangular coordinate system, the expectation value of the electron's position formula are given by

$$\langle x \rangle = \int_0^{L_x} \Psi_n^*(x,t)\, x\, \Psi_n(x,t) dx = \frac{2}{L_x} \int_0^{L_x} x \left(\sin^2\left(\frac{n_x \pi}{L_x} x\right)\right) dx = \frac{L_x}{2} \tag{24}$$

$$\langle z \rangle = \int_0^{L_z} \Psi_n^*(z,t)\, z\, \Psi_n(z,t) dx = \frac{2}{L_z} \int_0^{L_z} z \left(\sin^2\left(\frac{n_z \pi}{L_z} z\right)\right) dz = \frac{L_z}{2} \tag{25}$$

Equation (24) and (25) show the average position of the electron is at the center of the 2D nano-MOSFET.

When the energy of the electron is E, the de Broglie wavelength is expresses as

$$\lambda_e = \frac{h}{\sqrt{2m^*E}} \tag{26}$$

Where *h* is the Planck's constant. The silicon lattice constant is 0.543nm. Nano-MOSFET certainly exhibits quantum effect when λ_e of electron is greater than silicon lattice constant. Not every object can behave like wave because of the very small value of Planck's constant. Since *h* is very small, the mass *m* of the objects must be very small so that the de Broglie wavelength is large enough to enable the objects to interact with their physical systems with wave nature. In this simulation project, nano-MOSFET is in the nanometer dimension, therefore the de Broglie wavelength should be in nanometer value. The very small mass of electron $9.109\text{x}10^{-31}$kg can enable wave behavior in this nano-MOSFET. On the other hand, extremely heavier objects, for instance basket ball, will be unable to exhibit wave effects.

For an electron of mass m in an equilibrium condition, the Schrödinger equation is

$$i\hbar \frac{\partial \Psi(\mathbf{r},t)}{\partial t} = \left(-\frac{\hbar^2}{2m}\nabla^2\right)\Psi(\mathbf{r},t) \tag{27}$$

According to reference [6], the product form of the wavefunction is given by

$$\Psi(\mathbf{r},t) = \psi(\mathbf{r})g(t)$$

where $g(t) = e^{-iEt/\hbar}$

Substituting the wavefunction product into equation (27) results in

$$\left(-\frac{\hbar^2}{2m}\frac{1}{\psi(\mathbf{r})}\nabla^2\psi(\mathbf{r})\right) = i\hbar\frac{1}{g(t)}\frac{\partial g(t)}{\partial t} \tag{28}$$

Equation (28) can be used to explain the effects of temperature on oscillations in electron density distribution. The left hand side of equation (28) is function of position (spatial) but not time, while the right hand side is a function of time but not position. This situation arises only when each side is equal to the same constant called E (energy). So,

$$\left(-\frac{\hbar^2}{2m}\nabla^2\psi(\mathbf{r})\right) = E\psi(\mathbf{r}) \tag{29}$$

$$i\hbar\frac{\partial g(t)}{\partial t} = Eg(t) \tag{30}$$

There are two operators for quantum mechanics; firstly is the momentum operator which is related to spatial part of a plane-wave function by

$$\psi(\mathbf{r}) = Ae^{\mathbf{ikr}}$$

and after applying the operator

$$\hat{o} = -i\hbar\frac{\partial}{\partial \mathbf{r}} \tag{31}$$

to function $\psi(\mathbf{r})$ leads to

$$-\mathrm{i}\hbar\frac{\partial}{\partial \mathbf{r}}\,\psi(\mathbf{r}) = -\mathrm{i}\hbar\frac{\partial}{\partial \mathbf{r}}\,\mathrm{A}\mathrm{e}^{\mathbf{ikr}} = \hbar\mathbf{k}\psi(\mathbf{r}) = \mathbf{p}\psi(\mathbf{r}) \tag{32}$$

where$\mathbf{p} = \hbar\mathbf{k}$ is the momentum. Hence equation (31) is called the momentum operator, expressed as

$$\hat{\mathbf{p}} = -\mathrm{i}\hbar\frac{\partial}{\partial \mathbf{r}}$$

Secondly, there is energy operator which is

$$\hat{\mathrm{E}} = \mathrm{i}\hbar\frac{\partial}{\partial \mathrm{t}} \tag{33}$$

Consider the temporal dependence of g(t)

$$\mathrm{g}(\mathrm{t}) = \mathrm{e}^{-\mathrm{iEt}/\hbar} \tag{34}$$

obtaining

$$\hat{\mathrm{E}}\mathrm{g}(\mathrm{t}) = \mathrm{i}\hbar\frac{\partial}{\partial \mathrm{t}}\mathrm{g}(\mathrm{t}) = \mathrm{i}\hbar\frac{\partial}{\partial \mathrm{t}}\mathrm{e}^{-\mathrm{iEt}/\hbar} = \hbar\frac{\mathrm{E}}{\hbar}\mathrm{g}(\mathrm{t}) = \mathrm{Eg}(\mathrm{t}) \tag{35}$$

In this paper, nanoscale devices are considered which operate using relatively large number of electrons. The above mathematical descriptions of such particles is given by solutions of Schrödinger equation as explained above.

3. Methodology

NanoMOS simulation tool is used for simulation study. Double-gate (DG) nano-MOSFET is used with all terminal biasing voltages set to zero, that is the device is simulated in equilibrium condition. In this simulation project, the material is silicon and wafer orientation is (001)/channel transport direction is [100]. The simulation temperatures studied are 77K and 300K. The electron transport models used include quantum model using Green's function approach and semiclassical model which is described by Boltzmann Transport Equation (BTE). The values of silicon body thickness are 1.0nm, 1.5nm and 2.0nm. Within these simulation settings, the particle-wave duality property of electron can be examined.

NanoMOS is a self-consistent 2D simulator for fully depleted, double-gate nano-MOSFETs. In thin-body silicon channel, Schrödinger equation is solved exactly in confinement direction. The self-consistent simulation coupled Poisson solver and transport model. In NanoMOS, only electron transport is considered and no hole transport is considered [17]. The channel length of the DG nano-MOSFET is fixed at 10nm so that ballistic transport can be investigated. The top and bottom gate contact workfunction are set to 4.188eV which is Al (aluminium) on SiO_2 (silicon dioxide). The top and bottom relative dielectric constant is 3.9. The channel body relative dielectric constant is 11.7. The longitudinal relative electron mass ratio is 0.98 and the transverse relative electron mass ratio is 0.19. All these material settings are for silicon channel nano-MOSFET in nanometer regime so that quantum energy levels splitting are significant. In thin body nano-MOSFET, essentially only the lowest subband is occupied by electrons. Therefore, it is sufficient to

consider only the lowest subband in order to study electron transport. Some references which used NanoMOS are listed in reference [18,19].

4. Results and Discussion

In this simulation project, all biasing voltages are set to zero volts. Figure 2 shows the 1st unprimed subband energy along the channel at equilibrium condition for various silicon channel thickness T_{Si} at 300K with ballistic transport using Green's function approach. From Figure 2 and Table 1, as T_{Si} decreases, potential barrier height increases. This situation causes more backscattering electrons and so lesser electrons will flow to the channel for thinner T_{Si}. Therefore, 2D electron density distribution in the channel will also be smaller for thinner T_{Si}. Also, steeper slope can be observed in the semilog plot of 2D electron density for thinner T_{Si}. Figure 3 exhibits this phenomenon.

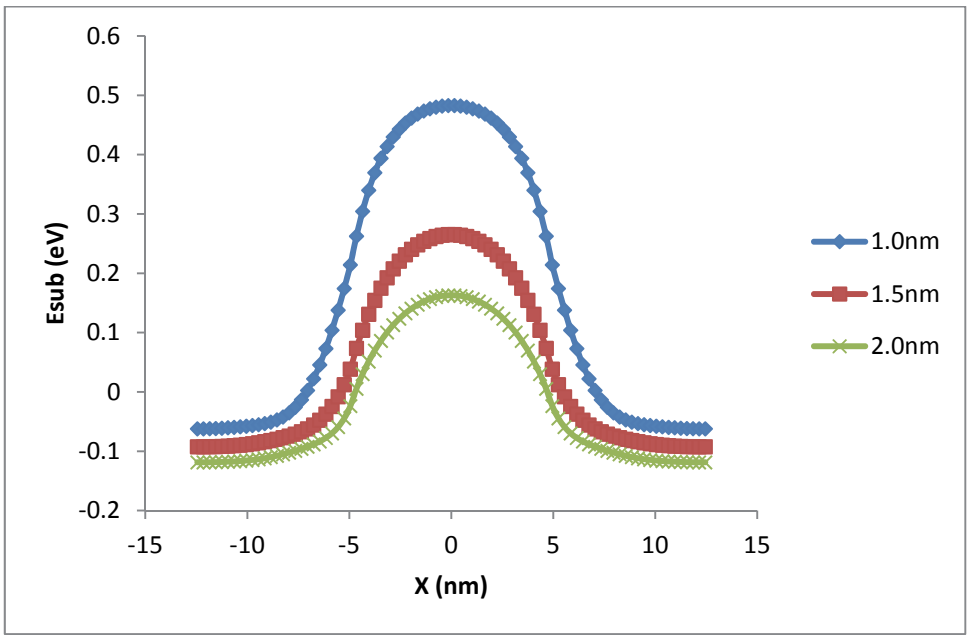

Fig. 2: 1st unprimed subband energy along the channel at equilibrium condition for various silicon channel thickness T_{Si} at 300K with ballistic transport using Green's function approach.

Table 1: This table shows silicon channel thickness values and their corresponding 1st unprimed subband energy as well as de Broglie wavelength

Thickness (nm)	1st unprimed subband energy at middle of the channel (eV)	de Broglie Wavelength (nm)
1.0	0.50	1.752
1.5	0.27	2.384
2.0	0.16	3.097

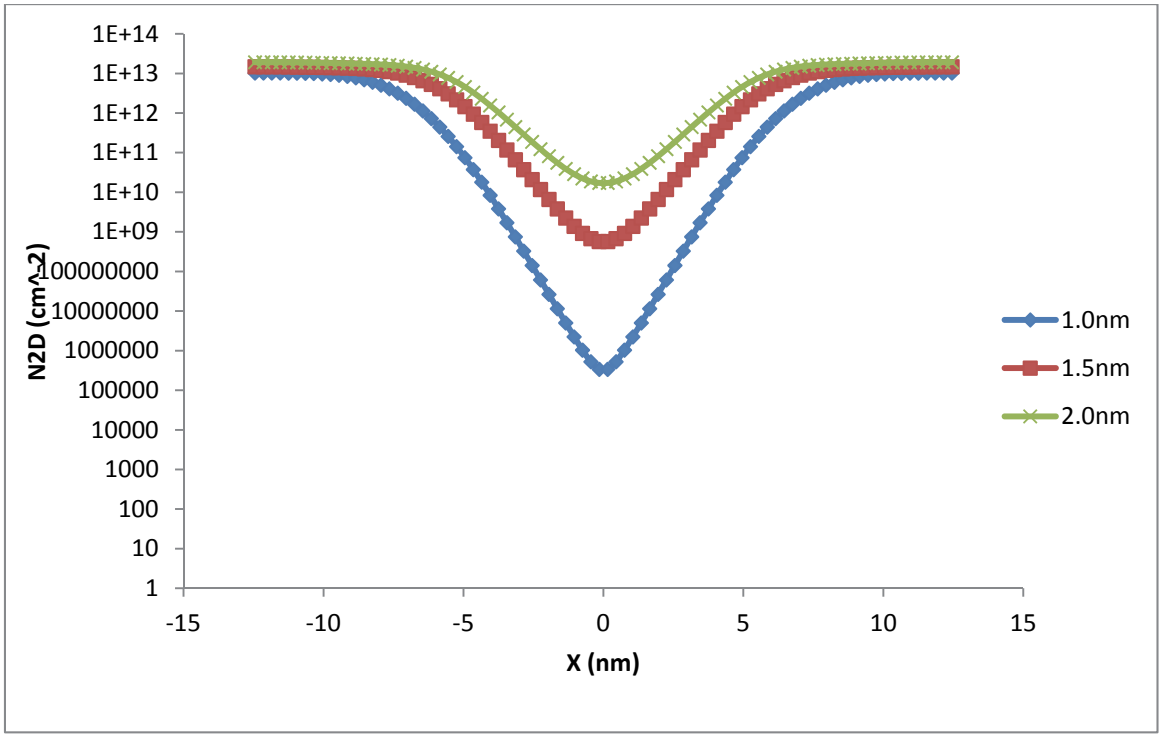

Fig. 3: Semilog plot of 2D electron density along the channel for various silicon channel thicknesses at 300K 1st unprimed subband energy.

From Figure 2 and Figure 3, in the channel region, T_{Si}=2.0nm has the lowest 1st unprimed subband energy and so this subband is the most populated with electrons. Thus, its 2D electron density is the highest among all the thicknesses studied. The channel region has less electron density than source/drain regions because the probability of electron to overcome the subband is become lesser and lesser. Energy of electrons in equilibrium condition without voltage biasing comes from thermionic emission.

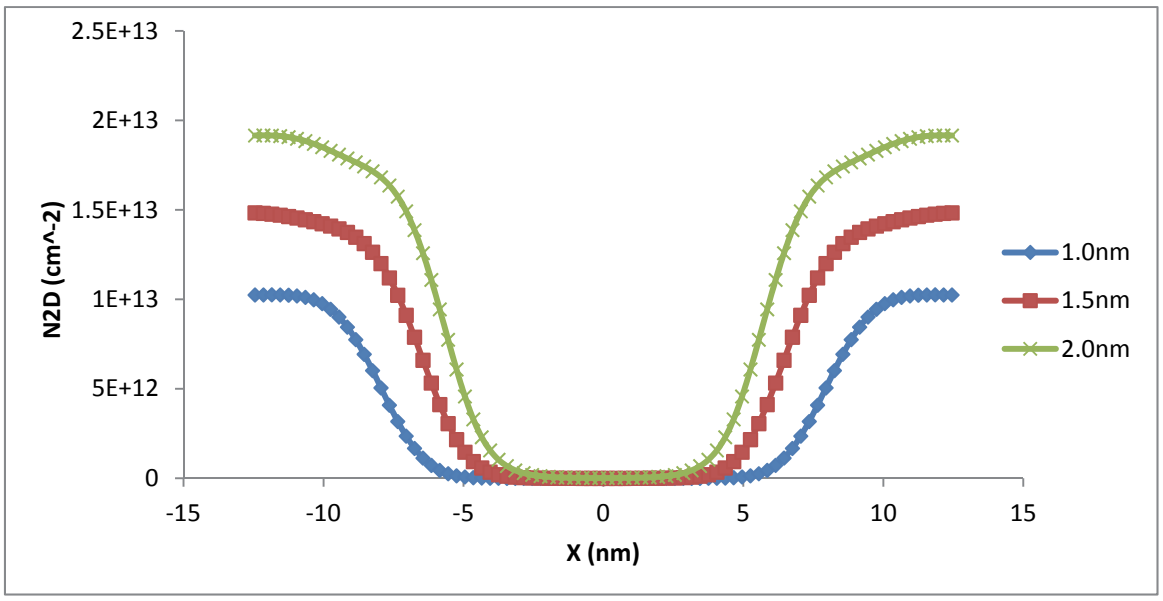

Fig. 4: Normal plot of 2D electron density along the channel for various silicon channel thicknesses at 300K 1st unprimed subband energy.

At source and drain contacts, when T_{Si} increases, 2D electron density n_i in source and drain contact increases (see Figure 4). When n increases, from equation (3), conduction band energy E_i (1^{st} unprimed subband energy) should reduce since energy of the Fermi level is fixed. So, thicker source/drain contacts have smaller energy level value as shown in Figure 2. With thinner T_{Si}, from Figure 4, 2D electron density at source/drain contacts reduces. From equation (3), E_i (1^{st} unprimed subband energy) should be higher.

When T_{Si} increases from 1.0nm to 2.0nm, n_i (for 1^{st} unprimed subband energy) in the channel increases by about 10^4 times (see Figure 3). Meanwhile, when T_{Si} increases from 1.0nm to 2.0nm, n_i (for 1^{st} unprimed subband energy) in the source/drain contacts increase only by 2 times (see Figure 4). This increase in n_i in source/drain contacts is not as significant as in the channel region because source/drain contacts are heavily N^+-doped with donor. As increment in n_i is smaller, from the relation $n_i \propto \left(\frac{E_F - E_i}{k_B T}\right) = \eta_0$, 1^{st} unprimed subbands energy value should be only different slightly in source/drain contacts with T_{Si} variations when compared with channel region where increment in n_i is larger (see Figure 2). So, the difference in 1^{st} unprimed subbands energy value should be more obvious in channel region (refer to Figure 2).

From Table 1, the de Broglie wavelength calculated using equation (26) for T_{Si} 1.0nm, 1.5nm and 2.0nm are all greater than silicon lattice constant 0.543nm. So, quantum effects are obvious in this DG nano-MOSFET with nanometer dimension.

From the theoretical section above, the average position of the electron should be located in the center of the 2D nano-MOSFET at rectangular coordinate position of $\frac{L_x}{2}$ and $\frac{L_z}{2}$, which corresponding to horizontal direction and vertical direction, respectively. However, from Figure 2, this center point has the highest potential barrier height so that 2D electron distribution at this point is the lowest (refer to Figure 3).

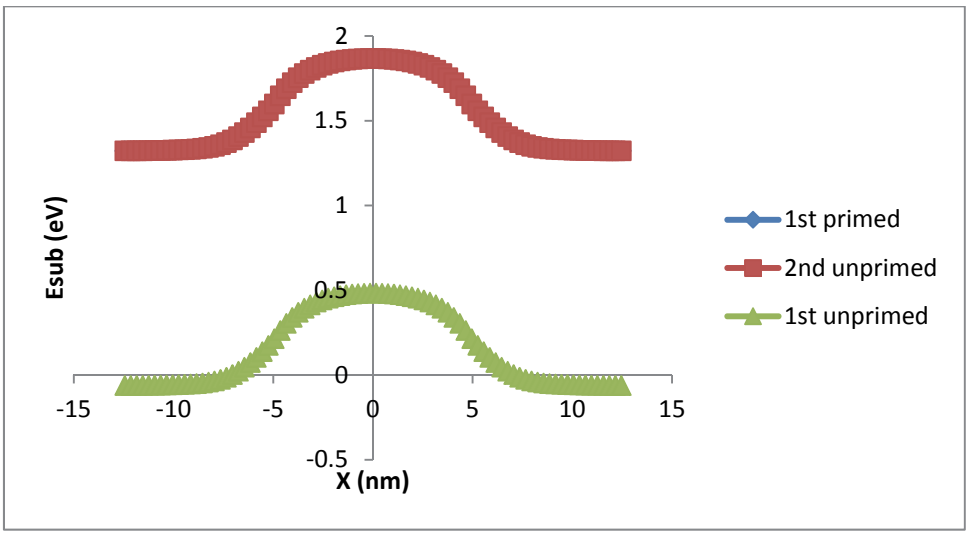

Fig. 5: Energy subbands profile along the channel for channel thickness 1.0nm.

Table 2: This table shows the silicon channel thickness values and the quantum energy levels splitting values

Thickness (nm)	Separation between energy levels (eV)
1.0	1.30
1.5	0.60
2.0	0.40

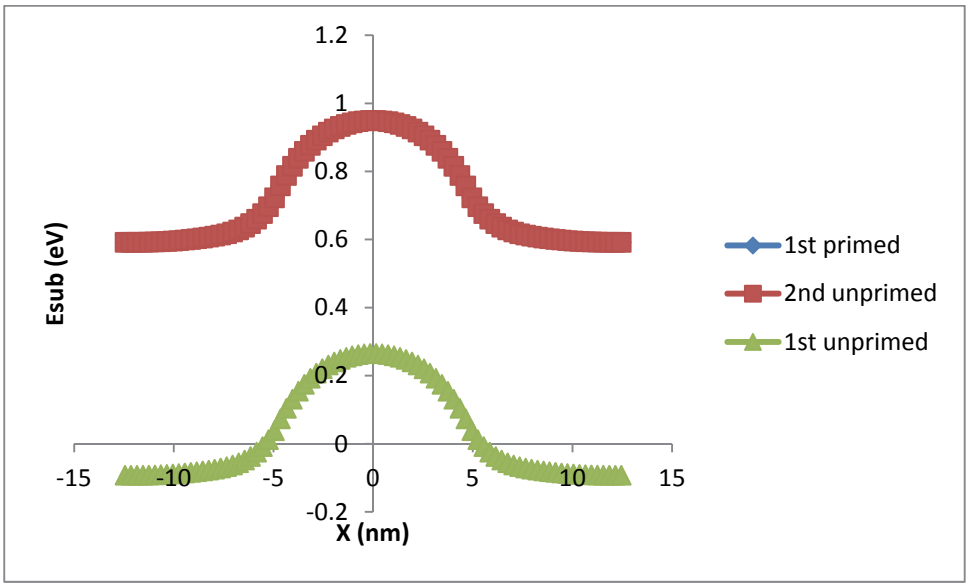

Fig. 6: Energy subbands profile along the channel for channel thickness 1.5nm.

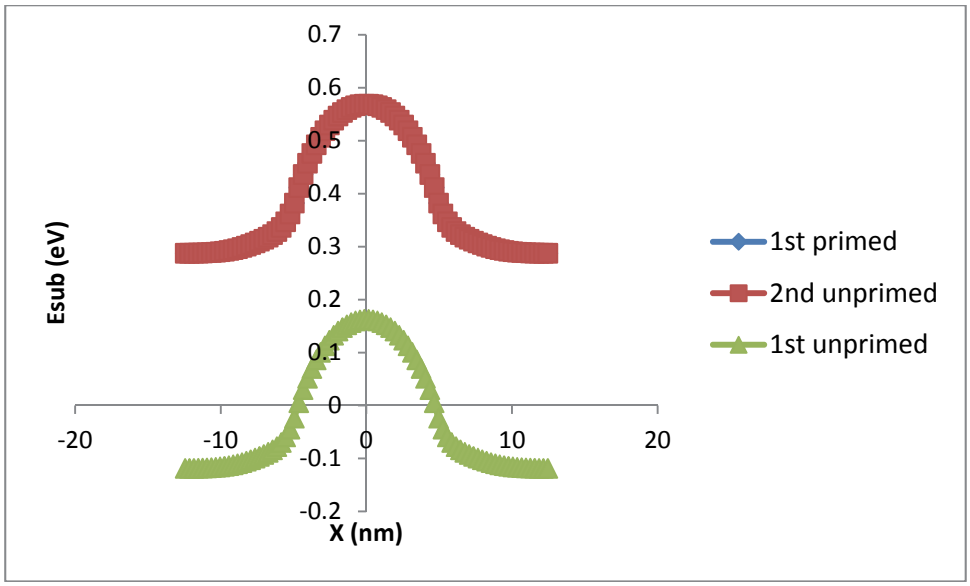

Fig. 7: Energy subbands profile along the channel for channel thickness 2.0nm.

Table 3: This table shows the simulated and calculated energy values for the three subbands energy levels at silicon channel thickness 1.5nm

Energy levels	**simulated energy (eV)**	**calculated energy (eV)**
1st unprimed subband	0.25	0.261
2nd unprimed subband	0.95	0.959
1st primed subband	0.95	0.899

Figure 5, Figure 6 and Figure 7 show the subbands energy profile for different T_{Si} with Green's function approach at 300K. Each figure has 1st and 2nd unprimed subbands as well as 1st primed subband. The 2nd unprimed has same energy as the 1st primed subband. Both of these two subbands have different quantum numbers. This phenomenon is called degenerate. As T_{Si} reduces, quantum splitting increases as shown in Table 2. Now, let compare the quantum energy levels between simulated data and theoretical calculation from equation (23). Let consider the case for channel thickness 1.5nm and Table 3 is obtained. In Table 3 theoretical calculation using equation (23), channel thickness is 1.5nm and channel length is 10nm. The electron effective mass for 1st and 2nd unprimed subbands is taken to be 0.98xfree electron mass whereas the 1st primed subband electron effective mass is lighter, which is taken to be 0.19xfree electron mass.

The chemical potential effects are included in the calculation for unprimed subbands. In this case, the theoretical formulae for the unprimed spacing between the two unprimed quantum energy levels for T_{Si}=1.5nm is given by

$$E_n - E_{n-1} = 0.261(2n - 1)\ \text{eV}$$

For unprimed subband in this case

$$E_2 - E_1 = 0.261(3)\ \text{eV} = 0.783\ \text{eV}$$

From simulation results in Table 3, it is equal to 0.700eV. The Fermi level is defined as the value of chemical potential at T=0K. Chemical potential is basically could be think as approximately the energy needed to add Nth electron to a system of N-1 electrons. So, in this simulation project, it can be related in 1st and 2nd unprimed subbands.

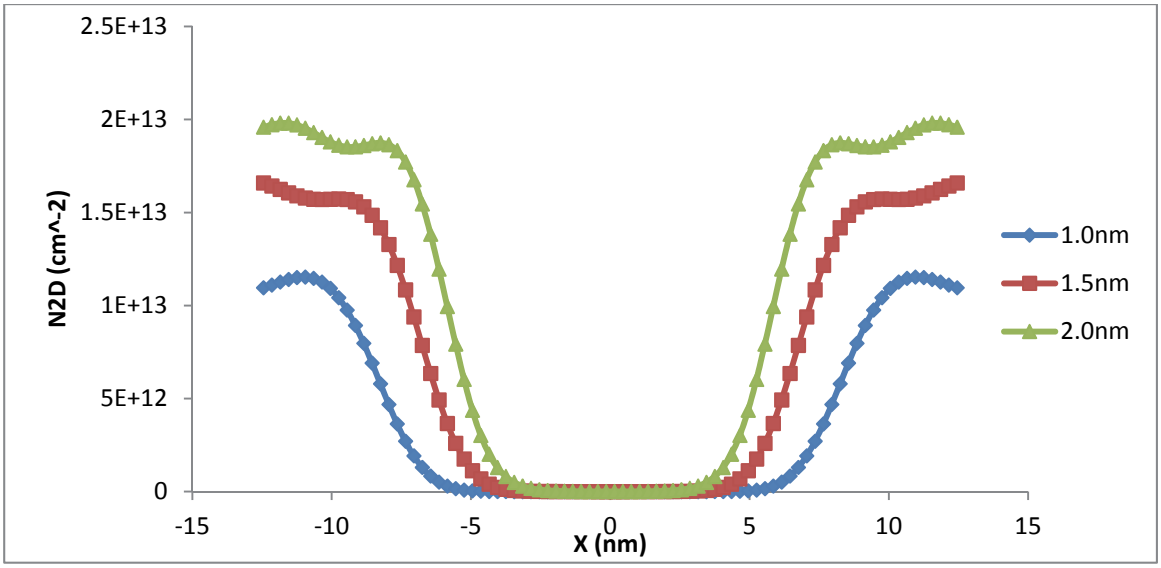

Fig. 8: Normal plot of 2D electron density along the channel for various silicon channel thicknesses at 77K using quantum model.

Figure 8 shows the 2D electron density distribution for various T_{Si} at 77K using quantum model. Figure 8 shows some oscillations near source and drain regions where Figure 4 which is the same plot with same design parameters but simulated at 300K doesn't exhibit such oscillations. In Figure 8, T_{Si} = 1.0nm curve indicates less wave oscillation nature in source/drain regions compared with T_{Si} = 2.0nm curve. This may due to quantum confinement effect where T_{Si} = 2.0nm has transition between bands because the energy bands are close to each other. Put in other words, as T_{Si} increases with constant thermal velocity, wavelength of the electron wave reduces and thereby coherence time reduces. The current challenge faced during designing quantum computer architecture is to scale the quantum computer to very large sizes where computational errors usually caused by decoherence as stated in reference [20].

In Figure 4 and Figure 8, as temperature increases, energy of electron increases, so does the velocity of electron. This causes the momentum of the electron increases. Momentum operator is position related as shown in equation (32). Hence, electron behaves more like particle in higher temperature 300K and thus oscillation patterns are not observed at high temperature.

In Figure 4 and Figure 8, as temperature reduces, energy of electron reduces. So, the effects of temporal dependence of energy in g(t) increases, which can be related by equation (34). Thus, electron behaves more as wave plane in low temperature 77K and thereby oscillation patterns are observed in low temperature. This is the case of electron has a particle-wave duality property.

So, at cryogenic low temperature (77K), electrons behave like wave which has interference effects. Meanwhile, high temperature destroys phase coherence which is important for quantum computing since computation must be completed before quantum states decohere.

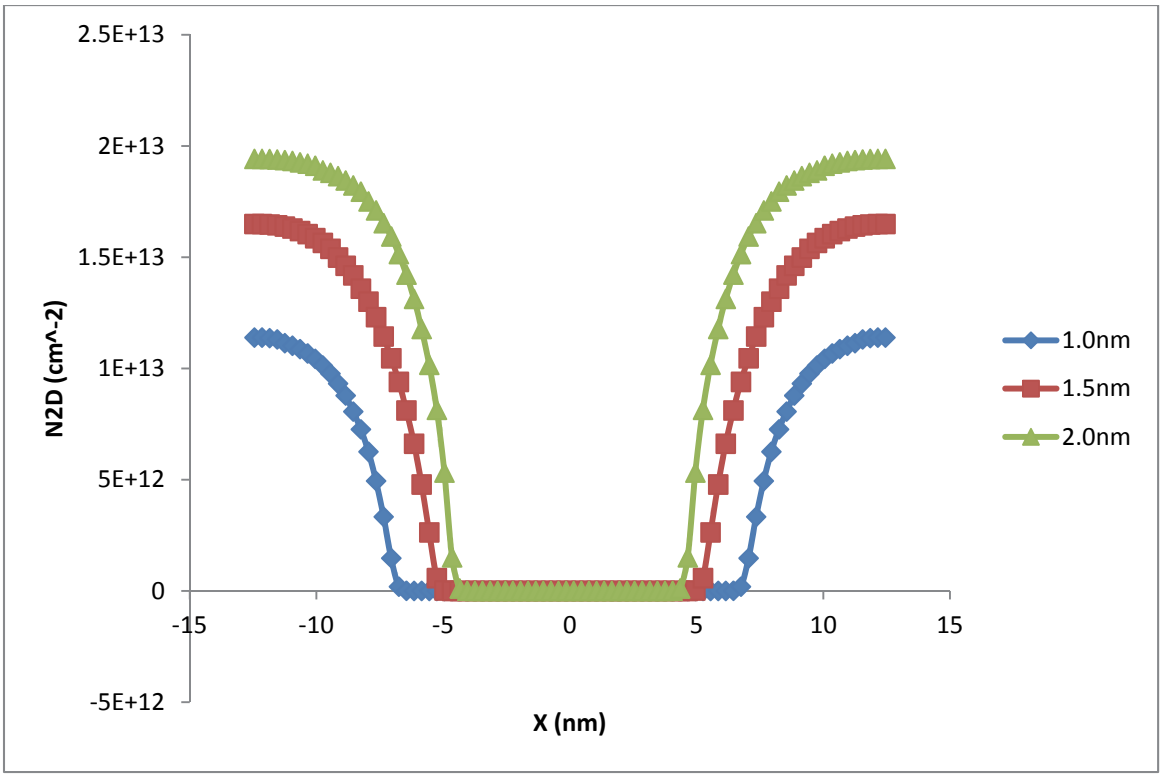

Fig. 9: Normal plot of 2D electron density along the channel for various silicon channel thicknesses at 77K using semiclassical model.

Put in other words, quantum charge density exhibits oscillations caused by interference of incident and reflected electron waves near source/drain regions at low temperature 77K. However, at high temperature when Poisson equation is used to solve for potential, the charge oscillations disappear, resulting in smooth profile. In semiclassical model (see Figure 9) no such oscillations are observed even at low temperature 77K since semiclassical model considered particle nature of electron through Boltzmann Transport Equation (BTE).

In this paper, nano-MOSFET in equilibrium condition is simulated whereas non-equilibrium condition is studied in references [21,22]. In this paper, quantum ballistic transport is mathematically described and simulated by Schrödinger-Poisson system by using Green's function approach whereas quantum ballistic transport in nanodevices is simulated using Asymptotic Waveform Evaluation (AWE) technique as in reference [23]. In this paper, nano-MOSFET structural dimensions are in nanometer regime whereas bulk MOSFETs, with 32nm technology node and 45nm gate length, are simulated to study temperature effects as in references [24,25].

5. Conclusion

In conclusion, the thinner the silicon channel of nanodevices, the more obvious the quantum energy levels splitting. At nanometer regime, quantum mechanics is essential for mathematical descriptions of quantum computer based on phosphorus donor atoms embedded in silicon lattice. The decoherence problem faced during scaling the quantum computer systems to very large size could be solved by operating the quantum computers at cryogenic temperature (extremely low temperature 77K) where electron-phonon collisions are reduced greatly. In nanodevices with quantum model electron transport, electrons

behave like wave at extremely low temperature and thereby quantum computer concept can be implemented. At room temperature, electrons lost wave nature and behave like particle. By this way, quantum computers may become reality by incorporating the silicon semiconductor technology used by current electronic industry.

References

[1] H. Vic Dannon, *Wave-Particle Duality: de Broglie Waves and Uncertainty*, Gauge Institute Journal **2** (4), November (2006)

[2] Greyson Gilson, *Unified Theory of Wave-Particle Duality, the Schrödinger Equations, and Quantum Diffraction,* Mulith Inc. (2014)

[3] R.E. Hummel, *Electronic Properties of Materials 4th edition,* DOI 10.1007/978-1-4419-8164-6_2, Springer Science (2011)

[4] Xufeng Wang, *NanoMOS 4.0: A Tool to Explore Ultimate Si Transistors and Beyond*. Purdue University, USA (2010)

[5] Zhibin Ren, *Nanoscale MOSFETs: Physics, Simulation and Design,* Purdue University, USA (2001)

[6] George W. Hanson, *Fundamentals of Nanoelectronics*, Pearson International Edition (2008)

[7] Hamish Johnston, *Computer Architecture Recreated on Quantum Device,* physicsworld.com (2011)

[8] Jeremy Hsu, *A Big Step Toward a Silicon Quantum Computer,* IEEE Spectrum (2013)

[9] V.C. Chan, T.M. Buehler, D.R. McCamey , R.G. Clark, *Single-Electron Transistor Coupled to a Silicon Nano-MOSFET,* Micro- and Nanotechnology: Materials, Processes, Packaging, and Systems II, Proc. Of SPIE Vol. 5650 (2005) DOI: 10.1117/12.583293

[10] Scott Aaronson, *The Limits of Quantum*, Scientific American, Inc. (2008)

[11] Amit Chaudhry, Jatindra Nath Roy, *Analytical Modeling of Energy Quantization Effects in nanoscale MOSFETs,* IJNeaM **5** (1) (2012) pp 1-9

[12] Amit Chaudhry, Jatindra Nath Roy, *Quantum Mechanical Direct Leakage Currents in a Sub 10nm MOSFET: A Rigorous Modeling Study,* IJNeaM **5** (1) (2012) pp. 39-46

[13] *Properties of Si, Ge, and GaAs at 300K,* siliconfareast.com (2004)

[14] M. De Michielis, D. Esseni, F. Driussi, *Trade-off between Electron Velocity and Density of States in Ballistic Nano-MOSFETs,* Udine, Italy (2004)

[15] Nouredine Zettili, *Quantum Mechanics: Concepts and Applications,* John Wiley & Sons Ltd, (2001)

[16] Michael A. Nielsen, Isaac L. Chuang, *Quantum Computation and Quantum Information: 10th Anniversary Edition,* Cambridge University Press (2010)

[17] Xufeng Wang, *NanoMOS 3.5 First Time User Guide*, Purdue University, USA.

[18] Zhibin Ren, Ramesh Venugopal, Sebastien Goasguen, Supriyo Datta, Mark S. Lundstrom, *NanoMOS 2.5: A Two-Dimensional Simulator for Quantum Transport in Double-Gate MOSFETs,* IEEE Transactions on Electron Devices, **50** (9) (2003)

[19] Amr A. Ahmadain, Kenneth P. Roenker, Karen A. Tomko, *A Study of the Performance of Ballistic Nanoscale MOSFETs using Classical and Quantum Ballistic Transport Models,* IEEE (2006)

[20] C. Monroe, R. Raussendorf, A. Ruthven, K.R. Brown, P. Maunz, L.M. Duan, J. Kim, *Large-scale Modular Quantum-Computer Architecture with Atomic Memory and Photonic Interconnects,* American Physical Society (2014)

[21] Victor A. Sverdlov, Thomas J. Walls, Konstantin K. Likharev, *Nanoscale Silicon MOSFETs: A Theoretical Study,* IEEE Transactions on Electron Devices, **50** (9) (2003)

[22] Anisur Rahman, Jing Guo, Supriyo Datta, Mark S. Lundstrom, *Theory of Ballistic Nanotransistors,* IEEE Transactions on Electron Devices, **50** (9) (2003)
[23] Huang JZ, Chew WC, Tang M, Jiang L, *Efficient Simulation and Analysis of Quantum Ballistic Transport in Nanodevices with AWE,* IEEE Transactions on Electron Devices, **59** (2) (2012)
[24] Vandana Kumari, Manoj Saxena, R.S. Gupta, Mridula Gupta, *Simulation Study of Insulated Shallow Extension Silicon On Nothing (ISESON) MOSFET for High Temperature Applications,* Microelectronics Reliability **52** (2012)
[25] Vandana Kumari, Manoj Saxena, R.S. Gupta, Mridula Gupta, *Temperature Dependent Drain Current Model for Gate Stack Insulated Shallow Extension Silicon On Nothing (ISESON)MOSFET for Wide Operating Temperature Range,* Microelectronics Reliability **52** (2012)